The Intergalactic Medium: Overview and Selected Aspects

Tristan Dederichs
tristan.dederichs@uni-bielefeld.de

August 22, 2018

Contents

1 Introduction

At the current epoch, most of the baryonic matter and roughly half of the dark matter reside in the space between the galaxies, the intergalactic medium (IGM) [1]. At earlier times, the IGM contained even higher fractions of all matter in the universe: 90% of all primordial baryons at $z \geq 1.5$ and 95% of all dark matter at $z = 6$ [2, 1]. The ongoing research of the composition and evolution of the IGM is of great importance for the understanding of the formation of galaxies and tests of cosmological theories. However, the study of the IGM is complicated by the fact that the baryons contained in it can only be detected by their absorption signatures. Therefore, as A. A. Meiksin (2009) has put it, "the physical structures that give rise to the features must be modeled" [2].

I will start with a very brief overview of the early universe (up to the point where the term intergalactic started to be applicable), followed by an analysis of the most prominent feature of the IGM, the Lyman-alpha forest, both in observations and simulations. With the the missing baryon problem, a possible limitation to Lyman-alpha studies is considered. In a similar manner, the state of metals in the intergalactic space is examined and implications on the constraints of the nature of Dark Matter are investigated.

2 Early universe and reionization

Due to the physical conditions present in the immediate aftermath of the big bang, the primordial matter, consisting of hydrogen and helium, was completely ionized [1, 2]. At around $z \sim 1100$ or $t \approx 380000\,\mathrm{a}$ the universe had expanded and cooled enough for the cosmic gas to recombine and become neutral [1]. The first stars and subsequently galaxies began to form after $z \sim 20$, thus ending the dark ages [1].

The next major cosmic event was the reionization of hydrogen which took place between $z \sim 12$ and $z \sim 6$ [3]. This process is driven by radiation emitted from quasars (especially in the late stages of reionization) and population III stars [1]. Some publications also find that supernovae contribute to the reionization, albeit to a lesser extend than stars [4]. The exact reionization mechanisms of each of the possible sources are subject to ongoing research.

3 The Lyα forest

3.1 Observations

As the IGM is not completely ionized, there are still remaining clouds of neutral hydrogen between the galaxies. Lyman-alpha (Lyα) transitions occur in neutral hydrogen (H I) between the ground state and the first excited state, the rest wavelength of this spectral line is 1216 Å [5]. When the light of distant quasars passes through multiple intergalactic H I clouds at different redshifts, several distinct absorption lines are created, which can be identified in the spectrum and are known as the Lyα forest. This forest provides one of the most important sources for the study of the IGM [6]. The upper part of figure 1 shows the spectrum of three quasars at different redshifts. The Lyα forest and the Lyβ forest, which occurs at a rest wavelength of 1025 Å, are visible as absorbtion lines in the spectrum.

Like hydrogen, helium is another element that is present in the universe and (after galaxies formed) the IGM since the Big Bang, making it important for modelling [1]. Singly ionized helium (He II) also exhibits Lyα absorption with a spectral line at 304 Å in the rest frame of the absorbing gas [7]. The Lyα forest that is formed by He II is harder to observe, because of foreground absorption of neutral hydrogen. As a result, only a few (1% at $z \sim 3$) quasars have enough transmission in the He II Lyα forest to be seen in the spectrum [1].

The Lyα forest is especially distinctive in the intermediate redshift region ($z \sim 2 - 5$), getting more transmissive at lower redshifts until only a small portion (30±10 %) of the gas is seen in Lyα absorption at $z \sim 0$, therefore making it less useful as a tool for lower redshifts. At higher z the absorbers blend into each other so that regions of near zero transmission are interrupted by small clearings, whereas at low z a near unity transmission is occasionally interrupted by a single absorber [8]. At even higher redshifts, the number of lines increases up to $z \sim 6$, where the forest then turns into the Gunn-Peterson trough, i.e. regions with no detected transmission, which is shown in the lower part of figure 1, hinting at a higher neutral hydrogen fraction at earlier times [9]. For helium this effect is even more apparent, because a very small amount of He II can lead to total absorption of the incoming radiation and produce a Gunn-Peterson trough, making the detection of the early stages of He II reionization difficult [7].

It should be noted, that the method of exploring the IGM via the emission of quasars is highly biased, as these objects clearly formed in overdense regions of the universe, which were also reionized earlier than the rest of the universe [10]. Additionally, the number of Lyα emitting galaxies observed at $z \geq 6$ is very limited compared to the intermediate redshift region [10].

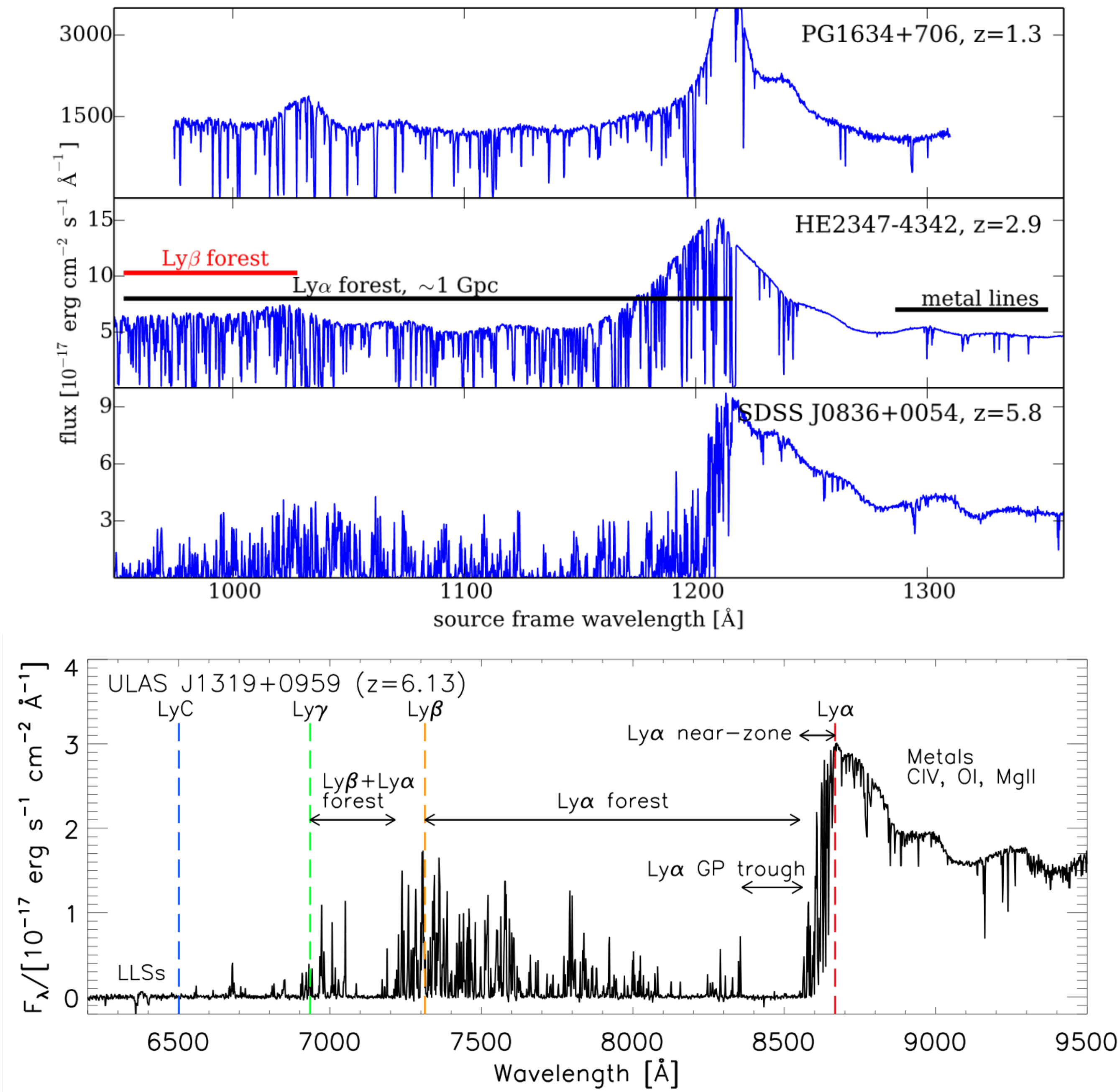

Figure 1: Lyα forest spectral region of quasars at different redshifts. **Top:** From X. Prochaska, Fechner and Reimers (2007), D'Odorico (2013) [1]. **Bottom:** From Becker and Bolton (2015) [3].

3.2 Simulations

Early simulations based on the λCMD model done by Davé, Hernquist, Katz and Weinberg (1999) reproduce the behaviour of the observed forest at varying redshifts, for example the increase of absorption lines in the quasar spectrum at higher redshifts compared to lower redshifts (left part of figure 3). The evolution of the number of lines per unit redshift $\frac{dN}{dz}$ for different Dark Matter models can be seen in figure 2 and both observations and simulations show a break at $z \sim 1.7$ [9]. For higher redshifts, the evolution of $\frac{dN}{dz}$ is thought to be due to the expansion of the universe, because the physical density associated with a given overdensity drops as the universe expands and therefore the neutral hydrogen fraction drops too [9].

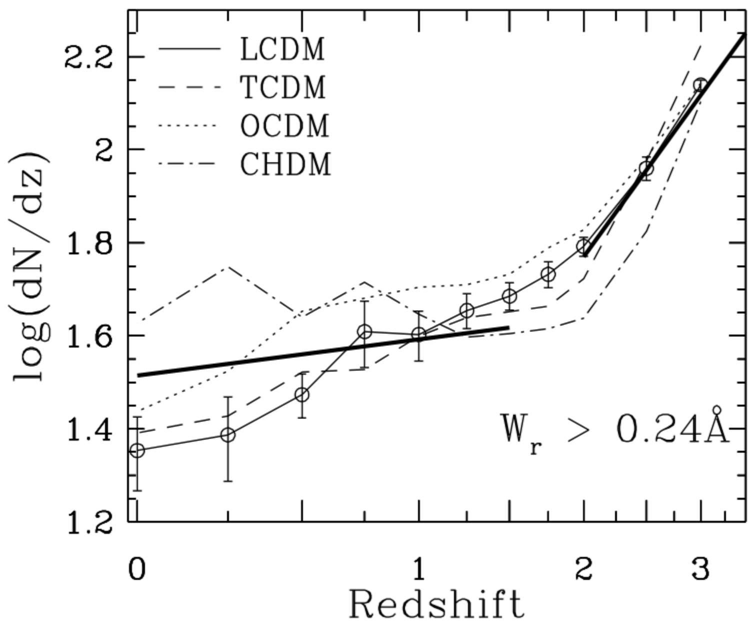

Figure 2: Evolution of the number of absorption lines per unit redshift $\left(\frac{dN}{dz}\right)$ in different CDM cosmologies (thin lines and data points with error bars) [9]. Thick solid lines are two separate observational data fits.

The simulations done by Weinberg et al. (2003) predict a Lyα forest that is qualitatively similar to the observed forest as well (right part of figure 3). The main parameters of the latter simulation are the density structures, the photoionization rates and the gas temperatures [1]. The statistical properties of the gas density field are modelled, as if the field evolved from the cosmological initial conditions by being ionized by a uniform background which is turned on at $z \sim 10$ and under the assumption that galactic feedback processes, such as the enrichment of the IGM through elements from the galaxies, have no significant impact on the low density gas seen in the Lyα forest. As the mean free path of ionizing photons is much longer relative to the mean distance between sources, the H I photoionization rate Γ is assumed to be spatially uniform. The temperature is assumed to be a power-law function of the density. Often this power-law is parameterized in terms of the density in units of the cosmic mean Δ_b as $T(\Delta_b) = T_0\Delta_0^{\gamma-1}$ with T_0 and $\gamma - 1$ being parameters that are varied to fit the observations. Further, it is assumed that the Lyα forest absorption can be extracted well enough, so that metal line contamination, errors in the estimate of the quasar's intrinsic continuum and damping wing absorption do not interfere with the simulation.

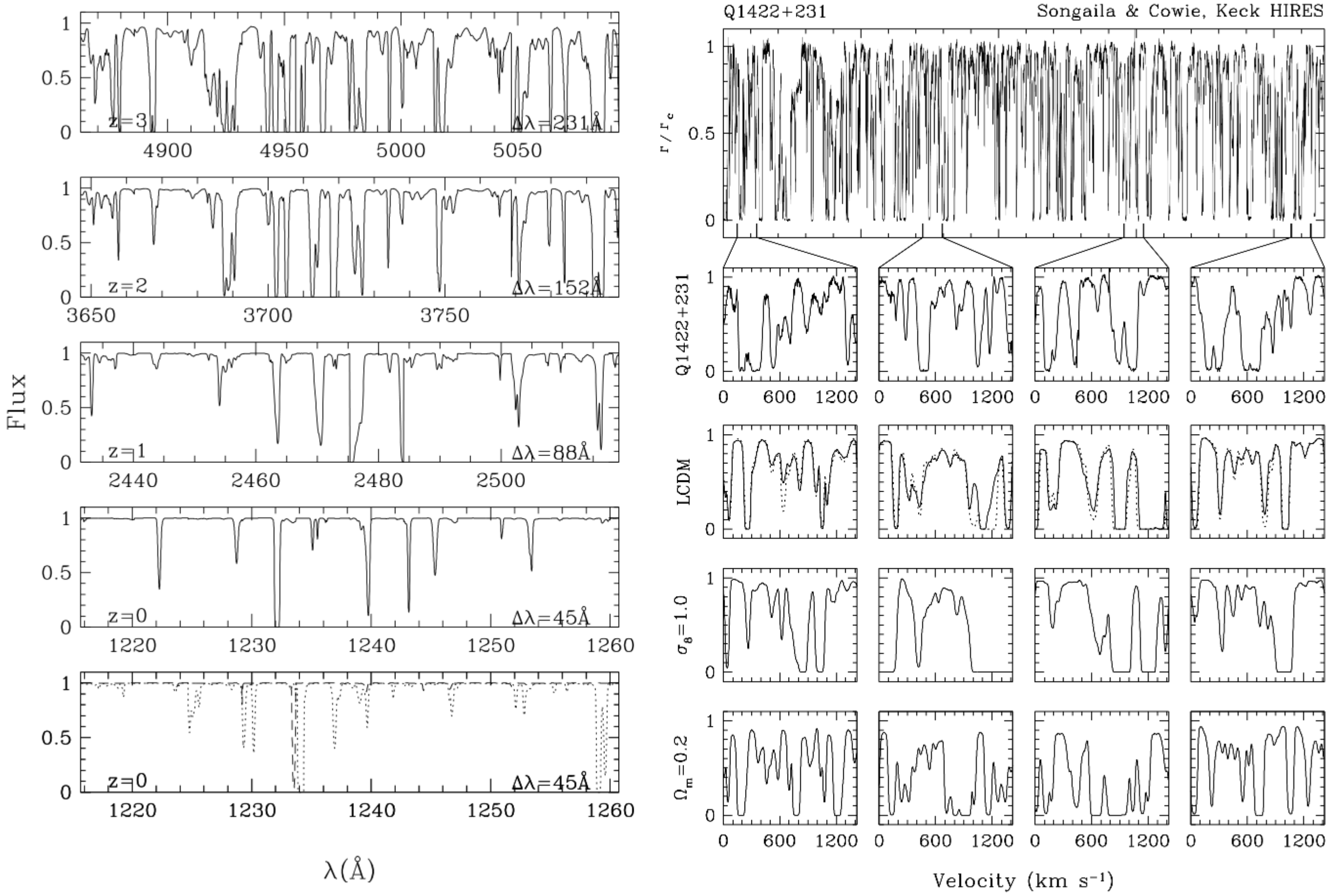

Figure 3: **Left:** Simulated Lyα spectra at different redshifts. The bottom panel shows simulated structure evolution scenarios discussed in the paper of Dave, Hernquist et al. (1999), [9]. **Right:** The two top rows show the continuum-normalized Lyα forest spectrum of quasar Q1422+231 with four regions zoomed in. The bottom three rows show the absorption in hydrodynamic simulations using three different cosmologies, varied from the ΛCDM case with $\sigma_s = 0.8$ and $\Omega_m = 0.4$ [1], from Weinberg et al. (2003).

Seljak et al. (2006) find that the predictions of simulations of the Lyα forest agree with the observed line-of-sight power spectrum $P_F(\equiv L^{-1}|\tilde{\delta}(k)|^2$, with $\tilde{\delta}(k)$ the Fourier transform of the overdensity in the transmission over a sight line L), also called the "normalized flux". The left panel of figure 4 shows the results of the simulation (lines) and observed data points with respective errors. Due to the high precision of the these measurements, important cosmological parameters like the matter density (Ω_m) can be constrained to 5-10%, providing an excellent way to test the consistency of ΛCDM models. Bolton et al. (2008) and Calura et al. (2012) find discrepancies between $2 \lesssim z \lesssim 3$ in the probability distribution function of transmission (TPDF). However, there is no tension regarding the TPDF between the data and a larger simulation done by Rollinde et al. (2013). Tytler et al. (2009) report that observations deviate by 10% from the simulations of the line-width distribution (line-width PDF), but the line-width distribution is reportedly very sensitive to the thermal history and is only crudely modeled in standard simulations anyway.

In conclusion, the models of the forest agree with the observations to $\sim$10% in the standard statistics. Through increased precision of the measurement and the use of new statistics, McQuinn (2016) thinks that further progress can be made in the future.

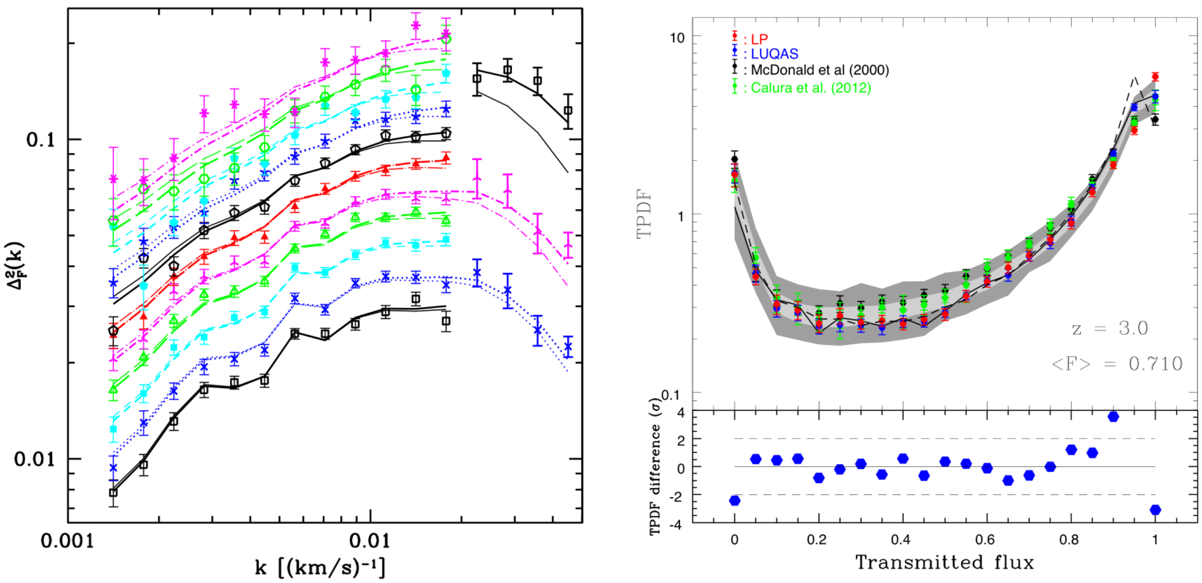

Figure 4: Two statistics applied to the Lyα forest [1]. **Left:** Power spectrum of the normalized flux $\frac{kP_F}{\pi}$ from Seljak et al. (2016). The points with the error bars are measurements of 3000 sloan quasar spectra for $k < 0.02\,\mathrm{s\,km^{-1}}$, the underlying curves are the predictions of the CDM model (thick curves) and of a model in which 6.5 keV sterile neutrinos are the Dark Matter (thin curves). The different colours are different redshifts, the lowest being $z = 2.2$ and the highest $z = 4.2$ in increments of $\Delta z = 0.2$. **Right:** The top panel shows the Lyα forest transmission probability distribution function (TPDF) at z = 3. The points with error bars show three measurements of this statistic, the solid curve is this statistic estimated from a simulation and the shaded regions represent 1σ and 2σ errors, from Rollinde et al. (2013). The bottom panel shows the residuals between the measurement and the simulations in units of the 1σ error.

3.3 The missing baryons problem

At lower redshifts the Lyα forest becomes progressively more transmissive as the universe is further diluted by cosmological expansion, with an average transmission of $\exp[-\tau_{\mathrm{eff}}]$ with $\tau_{\mathrm{eff}} = 0.016(1+z)^{1.1}$ over $0 < z < 1.2$, compared to $\tau_{\mathrm{eff}} = 0.36$ at z = 3. Estimates find that only $30 \pm 10\%$ of the $z \sim 0$ gas is seen in Lyα absorption and that $\sim 10\%$ of the baryons lie within galaxies or reside as hot gas inside galaxy clusters [1]. More precise studies find that Lyα absorbing material accounts for $29 \pm 4\%$ of the baryon content at $z < 0.07$ [11]. Therefore a large fraction of the baryons seems to be "missing", resulting in the "missing baryon problem" [1]. Cosmological simulations indicate that the missing baryons may reside throughout the filaments of the cosmic web (where matter density is larger than average) as a low-density plasma at temperatures of $10^5 - 10^7$ kelvin, known as the warm-hot intergalactic medium (WHIM). The WHIM is infamous for being hard to observe, X-ray observations may be used to study the hot gas, but are effective only in probing dense and hot regions, such as the central parts of galaxy systems, and not sensitive to the diffuse WHIM in which the bulk of the missing baryons are expected to reside [12]. Despite some progress in this area Shull et al. (2012) still report that 30% of all baryons are missing in their calculations.

Lim et al. (2017/2018) try to use the Sunyaev-Zel'dovich effect (SZE) to probe the WHIM. They argue, that when cosmic microwave background (CMB) photons pass through galaxy systems they are scattered by the free electrons in these systems resulting in a thermal and kinetic Sunyaev-Zel'dovich effect (tSZE and kSZE) [12]. By cross-correlating galaxy systems and their SZE in the CMB the authors hope to find a way to probe the WHIM associated with dark matter halos and the results indeed support the hypothesis, that all the missing baryons are contained in the WHIM.

4 Metal enrichment

4.1 Observations and simulations

Stars did not only ionize the IGM, but the radiation pressure of the stars, combined with supernovae action, powered winds that enriched the IGM with metals [1]. Metal-line absorption is different from the Lyα forest due to its much greater sensitivity to the processes of galaxy formation and evolution. While galactic outflows suppress star formation and therefore metal production, they concurrently distribute metals into haloes and the IGM [13].

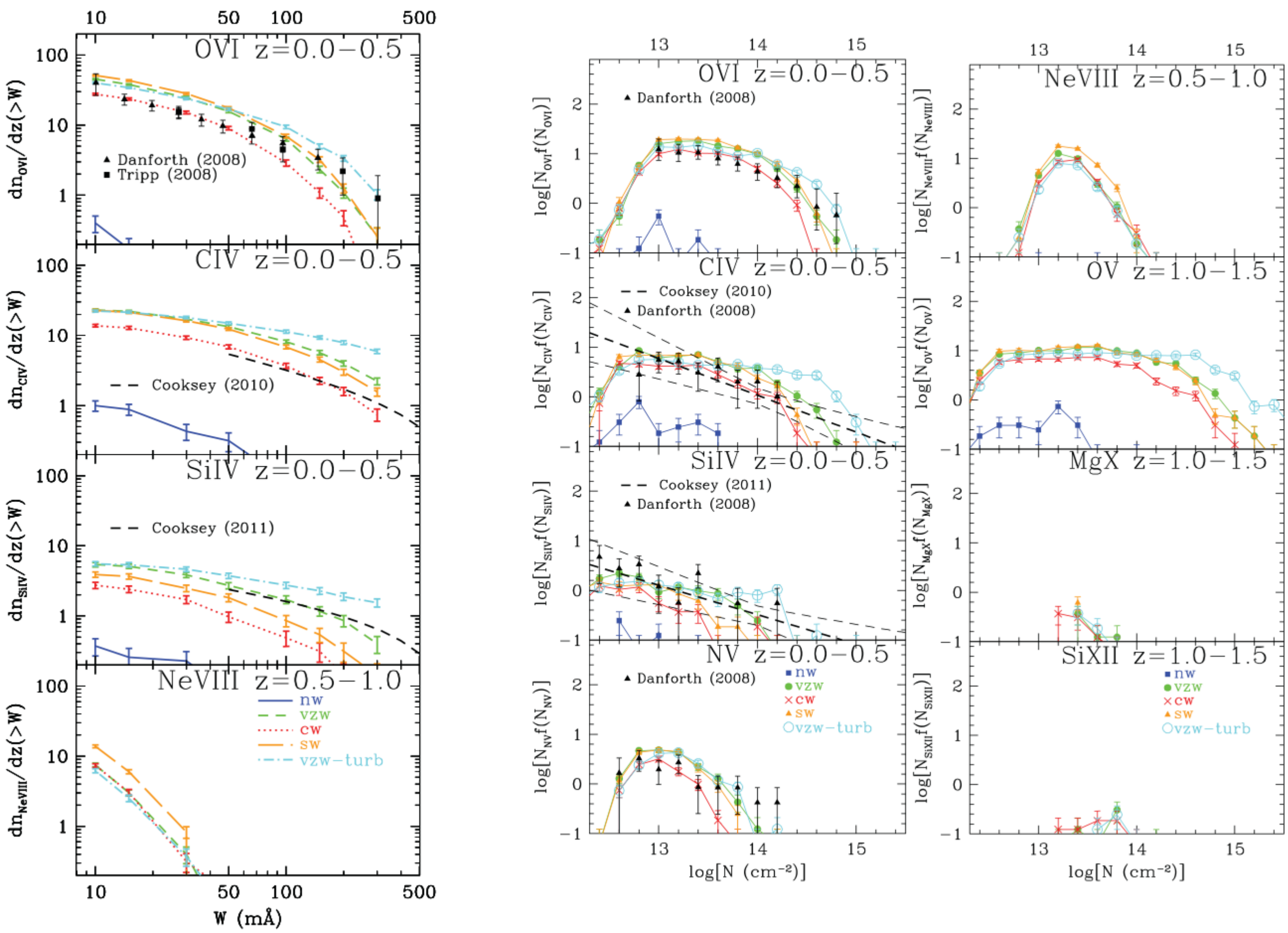

Figure 5: **Left:** Cumulative equivalent width distributions of four metals and different wind models from Oppenheimer, Davé et al. (2012) and measurements from Danforth and Shull (2008), Tripp et al. (2008) and Cooksey et al. (2010, 2011). **Right:** Simulated column density distributions with S/N = 30 for six metals and different wind models from Oppenheimer, Davé et al. (2012) and measurements from Danforth and Shull (2008) and Cooksey et al. (2010, 2011). [13]

Oppenheimer, Davé et al. (2012) have repeatedly tried to simulate the metal enrichment of the IGM, mostly concentrating on the $z \sim 0 - 2$ region. In their 110-million-particle cosmological hydrodynamic simulations it is assumed that every particle in a star-forming region has a probability of $p_{ej} = \eta \cdot \frac{SFR}{m_p}$ of being ejected from its galaxy with the velocity v_{wind}, where η is the mass-loading factor (which depends on the galaxy's internal velocity dispersion), SFR is the star formation rate and m_p is the particle mass. Different constraints of the factors of this formula result in different wind models. In the constant wind (cw) model, the velocity of ejected particles is constant with $v_{\text{wind}} = 680\,\frac{\text{km}}{\text{s}}$ and $\eta = 2$ for all galaxies. For the slow wind (sw) model $\eta = 2$ too, but $v_{\text{wind}} = 340\,\frac{\text{km}}{\text{s}}$, so only half as fast as for cw. In the momentum-conserved wind (vzw) model, v_{wind} is a function of the galaxy's

internal velocity dispersion (and hence the mass-loading factor) and the luminosity. The simulated results for these three models, together with the no wind (nw) model and the turbulent wind model, a variation of the vzw model, are shown in figure 5, where they are compared to measured data using the statistical methods of equivalent width distribution (EWD) and column density distribution (CDD).
The authors conclude that the "cw, vzw and sw wind models all predict $z < 0.5$ O VI observational statistics (EWDs, CDDs, cosmic ion densities) that agree within a factor of 2 with observations by the STIS and FUSE. By contrast, the nw model produces an O VI incidence 100 times lower than the other feedback models and observations. All wind models overproduce the C IV and Si IV incidence relative to available observations" [13]. In their favoured model (turbulent vzw), 20% of the metals are found outside of halos at $z \sim 2$, but only 4% at $z \sim 0$, therefore the majority of metals today reside within galaxies, in contrast to the bulk of baryons that reside outside haloes.

4.2 Dark Matter implications

Bremer, Dayal and Ryan-Weber (2018) examine the constraints that the metallicity of the IGM gives for different Dark Matter cosmologies. They use a semi-analytic model called Delphi (**D**ark Matter and the **e**mergence of ga**l**axies in the e**p**oc**h** of re**i**onization) [14]. It is based on the idea that 1.5 keV Warm Dark Matter (WDM) models have much less bound Dark Matter in low mass halos than Cold Dark Matter (CDM) models, therefore these halos have lower gravitational potential, resulting in less metals produced and distributed to the IGM. The model tracks the Dark Matter and baryonic assembly of galaxies at $z \simeq 4 - 20$ and can incorporate different assumptions on the nature of Dark Matter, such as CDM, 1.5 keV, 3 keV and 5 keV WDM models. The approach is to generate merger-trees for the dark matter halos (i.e. build large halos by merging small halos) and baryonic matter. For the latter the first progenitors of any halo are assigned a gas mass M_g that scales with the halo mass M_h through the cosmological ratio such that $M_g = \frac{\Omega_b}{\Omega_m} M_h$. A fraction of this gas mass is converted into stars, the lower limit on this star formation efficiency is given by the efficiency needed to produce enough type II supernovae. The initial mass function is taken from Salpeter (1955) and a fixed metallicity of $0.2\, Z_\odot$ is assumed, then the complete spectrum for each galaxy is generated using the stellar population synthesis code *Starburst99* from Leitherer et al. (1999, 2010). When testing the model against data sets, Bremer et al. find that the UV luminosity functions are consistent with CDM, 3 keV and 1.5 keV scenarios. All DM models seem to be consistent with observations of the stellar mass densities (see figure 6) and ejected gas mass densities. The fact that only bright galaxies with $M_{\mathrm{UV}} \leq -18$ are well observed poses a problem and the authors believe that galaxy magnitudes need to be measured down to at least $M_{\mathrm{UV}} = -16.5$ to distinguish between CDM and WDM scenarios. However, simulations done by Simcoe et al. (2011) rule out all models except CDM and 3 keV WDM at 1.6σ, leading Bremer et al. to suggest that by combining several models and data sets along with more precise UV measurements of galaxies it might be possible to rule out all Dark Matter candidates but CDM in the near future.

5 Conclusion

As the study of the IGM inevitably touches the field of cosmology, observations are usually scarce and the reliance on models and simulations is vital. The spectra of quasars contain information on the intergalactic space in the form of absorption lines of hydrogen and helium at different redshifts. The hydrogen Lyα forest is best studied in the intermediate redshift region $z \sim 2 - 5$ and after the break in the $\frac{dN}{dz}$ evolution at $z \sim 1.7$, Lyα forest models match observations statistically to $\sim 10\%$. The metallicity of the IGM at $z \sim 2-3$ is between $10^{-3.5}$ and $10^{-2.0}\, M_\odot$ [13], but it is currently not fully understood how the metals were distributed from galaxies to the IGM. However, it is possible to find constraints on the nature of Dark Matter from simulating and observing the metallicity of the IGM and galaxies.
In conclusion, most open questions are either related to the low redhift region $z \sim 0$, the high redshift region $z > 6$ or the connection between the IGM and galaxies and some of them may be answered by more elaborate (cf. WHIM) or preciser (cf. metallicity) measurements.

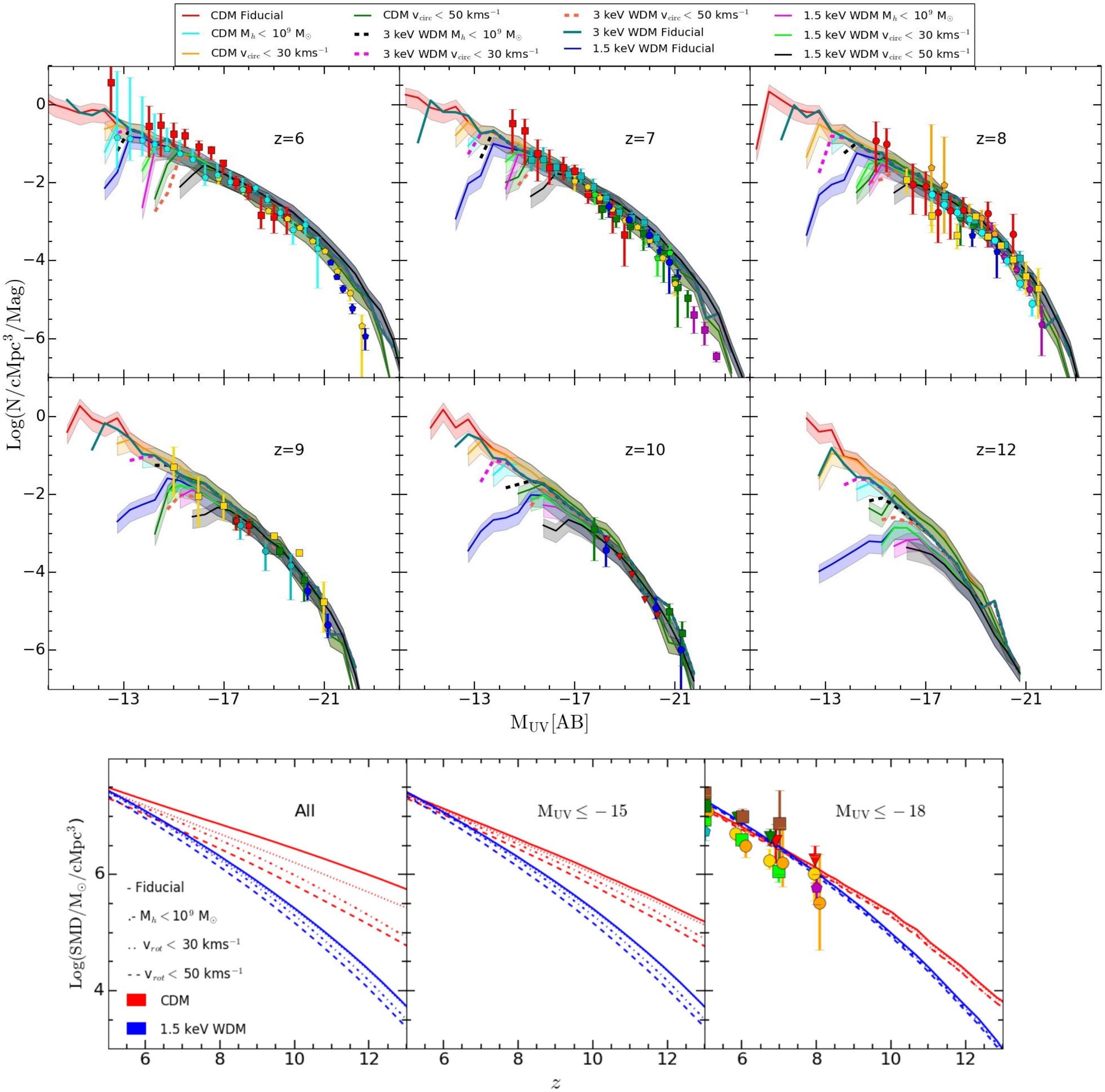

Figure 6: From Bremer, Dayal and Ryan-Weber (2018) [14]. **Top:** Number density of Lyman Break Galaxies as a function of the UV luminosity at $z \simeq 6-12$. Coloured lines indicate different DM models, the shaded regions show the $1-\sigma$ Poisson errors, points show observational data [14]. **Bottom:** Stellar mass densities (SMD) as a function of redshift for all galaxies (left panel), $M_{UV} \lesssim -15$ galaxies (middle panel) and $M_{UV} \lesssim -18$ galaxies (right panel). Coloured lines show different cosmologies and feedback models, points are SMD observations.

References

[1] M. McQuinn. The Evolution of the Intergalactic Medium. *Annual Review of Astronomy and Astrophysics, vol. 54, p.313-362*, 2016.

[2] A. A. Meiksin. The physics of the intergalactic medium. *Reviews of Modern Physics, vol. 81, Issue 4, pp. 1405-1469*, 2009.

[3] G. D. Becker, J. S. Bolton, and A. Lidz. Reionization and high-redshift galaxies: the view from quasar absorption lines. *Publications of the Astronomical Society of Australia, Volume 32, id.e045 29 pp.*, 2015.

[4] J. L. Johnson and S. Khochfar. The Contribution of Supernovae to Cosmic Reionization. *The Astrophysical Journal, Volume 743, Issue 2, article id. 126, 10 pp.*, 2011.

[5] B. Carrol and D. Ostlie. *An Introduction to Modern Astrophysics*. New York: Addison-Wesley Publishing Company, Inc., 1996.

[6] V. Irsic and M. McQuinn. Absorber Model: the Halo-like model for the Lyman-α forest. *Journal of Cosmology and Astroparticle Physics, Issue 04, article id. 026*, 2018.

[7] P. LaPlante, H. Tac, et al. Helium Reionization Simulations. III. The Helium Lyman-α Forest. *eprint arXiv:1710.03286*, 2017.

[8] A. Garzilli, T. Theuns, and J. Schaye. The broadening of lyman-alpha forest absorption lines. *Monthly Notices of the Royal Astronomical Society, Volume 450, Issue 2, p.1465-1476*, 2015.

[9] R. Dave and L. Hernquist. The Low Redshift Lyman Alpha Forest in Cold Dark Matter Cosmologies. *The Astrophysical Journal, Volume 511, Issue 2, pp. 521-545.*, 1999.

[10] M. Dijkstra. Ly α Emitting Galaxies as a Probe of Reionisation. *Publications of the Astronomical Society of Australia, Volume 31, id.e040 26 pp.*, 2014.

[11] J. Bregman. The Search for the Missing Baryons at Low Redshift. *Annual Review of Astronomy & Astrophysics, vol. 45, Issue 1, pp.221-259*, 2007.

[12] S. Lim, H. Mo, et al. The detection of missing baryons in galaxy halos with kinetic Sunyaev-Zel'dovich effect. *eprint arXiv:1712.08619*, 2017.

[13] B. D. Oppenheimer, R. Dave, et al. The intergalactic medium over the last 10 billion years - II. Metal-line absorption and physical conditions. *Monthly Notices of the Royal Astronomical Society, Volume 420, Issue 1, pp. 829-859*, 2012.

[14] Jonas Bremer, Pratika Dayal, and Emma Ryan-Weber. Probing the nature of Dark Matter through the metal enrichment of the intergalactic medium. *MNRAS, Volume 477, Issue 2, p.2154-2163*, 2018.